Title

Evaluation of Angioarchitectural Features of Unruptured Brain Arteriovenous Malformation by Susceptibility Weighted Imaging

Authors

Wu, Chun-Xue
Ma, Li
Chen, Xu-Zhu
et al.

Publication Date

2018-08-01

DOI

10.1016/j.wneu.2018.05.151

Peer reviewed

HHS Public Access

Author manuscript

World Neurosurg. Author manuscript; available in PMC 2019 November 25.

Published in final edited form as:

World Neurosurg. 2018 August ; 116: e1015–e1022. doi:10.1016/j.wneu.2018.05.151.

Evaluation of Angioarchitectural Features of Unruptured Brain Arteriovenous Malformation by Susceptibility Weighted Image (SWI)

Chun-Xue Wu, MD[1], **Li Ma, MD**[2,3], **Xu-Zhu Chen, MD**[1], **Xiao-Lin Chen, MD, PhD**[2,3], **Yu Chen, MD**[2,3], **Yuan-Li Zhao, MD, PhD**[2,3,4,5], **Christopher Hess, MD, PhD**[6], **Helen Kim, PhD**[6], **Heng-Wei Jin, MD**[7], **Jun Ma, MD**[1,*]

[1]Department of Radiology, Beijing Tiantan Hospital, Capital Medical University, No. 6 Tiantan Xili, Dongcheng District, Beijing, People's Republic of China 100050

[2]Department of Neurosurgery, Beijing Tiantan Hospital, Capital Medical University, No. 6 Tiantan Xili, Dongcheng District, Beijing, People's Republic of China 100050

[3]China National Clinical Research Center for Neurological Diseases, Beijing, People's Republic of China

[4]Stroke Center, Beijing Institute for Brain Disorders, Beijing, People's Republic of China

[5]Beijing Key Laboratory of Translational Medicine for Cerebrovascular Disease, Beijing, People's Republic of China

[6]Center for Cerebrovascular Research, Department of Anesthesia and Perioperative Care, University of California San Francisco, San Francisco, CA, USA

[7]Department of Interventional Neuroradiology, Beijing Tiantan Hospital, Capital Medical University, No. 6 Tiantan Xili, Dongcheng District, Beijing, People's Republic of China 100050

Abstract

* Corresponding author: Jun Ma; dr_ma@sina.com; Tel: +861067098182.

Disclosure paragraph:

1) The scientific guarantor of this publication is Jun Ma, Vice President of Department of Neuroradiology, Beijing Tiantan Hospital, Capital Medical University.

2) The authors of this manuscript declare relationships with the following companies:.

The authors of this manuscript declare no relationships with any companies, whose products or services may be related to the subject matter of the article.

4) No complex statistical methods were necessary for this paper.

5) Institutional Review Board approval was obtained.

6) *Only if the study is on human subjects:*

Written informed consent was obtained from all subjects (patients) in this study.

7) *Only if the study is on animals:*

No animal study in this work

8) None of the study subjects or cohorts have been previously reported.

9) Methodology:

• retrospective

• observational

• performed at one institution

OBJECTIVES—A precise assessment of angioarchitectural characteristics using non-invasive imaging is helpful for serial follow-up and weighting risk of natural history in uruptured brain arteriovenous malformation (bAVM). This study aimed to test the hypothesis that susceptibility weighted image (SWI) would provide an accurate evaluation of angioarchitectural features of unruptured bAVM.

METHODS—A total of 81 consecutive patients with unruptured bAVM were examined. Image quality of SWI for the assessment of bAVM angioarchitectural features were determined by a five-point scale. The accuracy of SWI for detection of angioarchitectural features was evaluated using DSA as a standard reference. And further compared among unruptured bAVMs with or without silent intralesional microhemorrhage on SWI to examine the potential confounding effect of microhemorrhage on image analysis.

RESULTS—All lesions were identified on SWI. Image quality of SWI was judged to be at least adequate for diagnosis (range, 3–5) in all patients by both readers. Using DSA as reference standard, the area under receiver operating curve (AUC) of detection of deep or posterior fossa location, exclusively deep venous drainage, venous ectasia, venous varices and the presence of associated aneurysm on SWI was 1, 0.93, 0.94, 0.95, and 0.83, respectively. Silent intralesional microhemorrhage were detected in 39 patients (48.15%) on SWI and no significant difference ($P > 0.05$) was found in angioarchitectural features between cases with and without silent microhemorrhage.

CONCLUSIONS—SWI might be a non-invasive alternative technique for angiogram in the angioarchitectural assessment of unruptured bAVM.

Keywords

Unruptured; Brain arteriovenous malformation; Susceptibility weighted image (SWI)

INTRODUCTION

Unruptured brain arteriovenous malformations (bAVM) have an annual risk for hemorrhage rate of 1.5%–3% and a risk of death at the time of first hemorrhage of about 10% that increases with each episode of repeat hemorrhage [1–5]. Certain angioarchitectural characteristics are considered to be associated with the risk of future hemorrhage, including posterior fossa or deep location, the presence of associated aneurysms, deep exclusive venous drainage, and venous stenosis or ectasia [1, 6–9]. Digital subtraction angiography (DSA) currently is the gold standard for diagnosis and follow-up of bAVM because of its high temporal and spatial resolution. However, it is not suitable for monitoring of unruptured bAVM because of risks including bleeding, allergy, nephrotoxicity, and thromboembolism, which add up to a risk of 0.1%–1% for permanent neurologic deficits[10–12]. Hence, many different studies have sought to develop non-invasive imaging method that avoid the risks associated with invasive procedures and offer more nuanced information regarding angioarchitectural features and repeated follow-up of bAVM.

Susceptibility weighted image (SWI) uses a fully flow-compensated, long echo gradient acquisition to highlight susceptibility differences between tissues [13]. SWI provides a natural separation of arteries and veins, making it possible to image both simultaneously and have

them be easily evaluated separately. Veins will be dark due to T2* losses, while arteries will be bright from time-of-flight inflow enhancement. Hemoglobin breakdown products show largely paramagnetic susceptibility. Hemoglobin breakdown products show largely paramagnetic susceptibility [14–16]. These properties form the basis for the ability of SWI to reveal unique features of bAVM not seen with other sequences. In view of the mentioned advantage of SWI, we hypothesized that SWI would be useful to detect certain angioarchitectural features of unruptured bAVM.

MATERIALS AND METHODS

This retrospective study was approved by our institutional review committee with waived informed written consent.

Patients and brain imaging

A total of 120 consecutive patients with a diagnosis of bAVM and undergoing brain MR examination and DSA at our institution were evaluated between January 2012 and March 2016. Initial presentation was classified as ruptured or unruptured. A bAVM was considered ruptured before diagnosis if there were signs of encephalomalacia adjacent to the lesion on MRI consistent with hemorrhage history based on previous radiological report[17]. Unruptured patients without treatment were included in this study. During this period, thirty ruptured patients and six patients undergone endovascular or surgical treatment were excluded. Finally, the study population consisted of 81 unruptured patients (35 females and 49 males; mean age, 30.47 years; range, 4– 75 years) with a mean time interval between MR imaging and DSA of 5 days (range, 2–13 days).

MR examinations included sagittal and axial T1WI, T2WI and SWI. MR images were acquired using 3.0 T clinical scanners (40 patients by Tim Trio, Siemens AG, Erlangen, Germany and 41 patients by Verio, Siemens AG, Erlangen, Germany), using the following protocols:

3T Tim Trio: T1WI: TR/TE=1600/9.4 ms, slice thickness =5 mm, FOV=512×432; T2WI: TR/TE=6000/97 ms, slice thickness =5mm, FOV =384×324; SWI: TR/TE =27/20 ms, slice thickness =2.5mm, flip angle =20^0, FOV=256×192. 3T Verio: T1WI: TR/TE=1600/9.4 ms, slice thickness =5 mm, FOV=512×496; T2WI: TR/TE=6000/97 ms, slice thickness =5 mm, FOV =640×640; SWI: TR/TE =27/20 ms, slice thickness =2.5mm, flip angle =20^0, FOV=512×384.

Cerebral angiography was performed using a DSA system (Allura Xper FD 20, Philip/Artis zee floor, Siemens AG/Innova IGS 630, GE). For each subject, a 5F angiographic catheter (Cordis) was selectively guided (150cm guide wire, Terumo) into bilateral internal carotid, external carotid and vertebral arteries respectively. The frame rate was 4/s in the arterial and 3/s in the venous phase. In addition, faster angiographic series (8 frames per second) were obtained to improve the result of cerebral AVM enhancement.

Image Analysis

Conventional angiograms were reviewed separately in a randomized order by one neurosurgeon (H.W., 7 years of experience). In all included patients, the angioarchitectural characteristics including the presence of associated aneurysm, deep exclusive venous drainage, venous stenosis or ectasia were included in the analysis. In addition, arterial feeders of the bAVM were evaluated. In all patients, axial T2-weighted images were available for DSA reading to enable better localization of the nidus. The location of nidus including posterior fossa (brainstem, cerebellum, or both) or deep locations (basal ganglia, thalamus, cerebellum, and corpus callosum) was recorded. The largest diameter (in millimetres) among the three dimensions was recorded as the maximal bAVM size for further analysis.

Venous ectasia was coded as positive in patients with a draining vein caliber ≥ two fold in relation to the normal vein on the contralateral side [18]. Venous pouches (varices) were defined as focal aneurysmal dilatations of the proximal draining vein.

Associated aneurysms were divided into 2 large subgroups: intranidal aneurysms and flow-related aneurysms. Intranidal aneurysms were located within or in the immediate vicinity of the nidus of bAVM. Flow-related aneurysms include aneurysms of vessels supplying the bAVM and aneurysms of the circle of Willis origin of an artery supplying blood to the nidus. Only associated aneurysms were included [19].

Two experienced neuroradiologists (both with > 7 years experience) who were blinded to clinical histories and the results of DSA reviewed SWI in a random order at a separate workstation (View- forum; Neurosoft Medical Systems). The judgement of intranidal microhemorrhage was assessed on SWI.

The presence of microhemorrhage was defined as signal loss consistent with hemosiderin [6]. Some other conditions (such as microhemorrhage or cortical petechial or intraventricular hemosiderosis observed in other parts of brain) were excluded. Some bAVM are associated with calcification, which is hard to diffirentiate from intralesional microhemorrahge. In these cases, CT could be used to help identify calcium. For the cases without CT examinations, the information from the magnitude images and the filtered phase images on SWI was combined to visualize calcification. On SWI scans, calcifications were identified according to the following parameters: hypointense signal on magnitude images and a hypointense signal on phase images.

To prevent recall bias, the interval between DSA and SWI was at least 4 weeks. Both readers individually evaluated the following features for qualitative analysis utilizing a five-point scale (5 = excellent, 4 = good, 3 = moderate, 2 = poor, and 1=non-diagnostic vessel delineation): delineation of (1) nidus, (2) feeder(s), (3) draining vein(s), and (4) overall image quality and presence of artifacts.

Any discrepancies between readers in detecting angioarchitectural characteristics and silent microhemorrahge after independent interpretation were resolved by consensus.

Statistical Analysis

The Kendall *W* coefficient of concordance was computed to compare the two readers in their assessment of image quality of SWI. Kendall *W* coefficients (K) of 0.5–0.8 were considered to indicate good agreement, and coefficients > 0.8 were considered to indicate excellent agreement.

The accuracy of SWI for the detection of angioarchitectural features were calculated by using the area under receiver operating curve (AUC) with DSA as reference standard. In addition, sensitivity, specificity, predictive positive value and negative predictive value were calculated.

The age at scan, the gender, and angioarchitectural characteristics between cases with and without microhemorrahge detected by SWI were compared using 2-sided, 2-sample *t* tests for continuous variables and Fisher exact tests for categorical variables.

A *P* value of < 0.05 was considered to indicate a significant difference. All statistical analyses were performed with software MedCalc 12.1 (MedCalc software; Mariakerke).

Results

Patients characteristics and DSA findings

Apart from 4 asymptomatic patients, symptoms included coma, headache, seizures and walking inability. Among the 81 included patients (35 females and 49 males; mean age, 30.47 years; range, 4– 75 years), the average maximal nidus size was 38.04 ± 12.03 mm. A total of 32 (39.50 %) lesions in these patients were in the deep or posterior fossa location, and 25 (30.86%) were identified with exclusively deep venous drainage by DSA. DSA revealed three associated aneurysms (3.70 %) in 3 patients.

Image quality of SWI for demonstration of angioarchitectural features in bAVM

SWI enabled clear depiction of arterial feeders and angioarchitectural risk factors in bAVM in accordance with DSA results. Image quality of SWI was judged by both readers to be excellent (score of 5), good (score of 4), or adequate for diagnosis (score of 3) in all patients. Image quality was not impaired by flow artifacts or areas of limited signal-to- noise ratio in any study. The average image quality score as judged by reader 1 was 4.2±0.4 (range, 3–5) and that as judged by reader 2 was 4.5±0.7 (range, 3–5), which yielded excellent interobserver agreement (K = 0.92, *P* =.023).

Accuracy of SWI for the Detection of angioarchitectural features in bAVM

With DSA as reference standard, SWI yielded a high diagnostic accuracy for each angioarchitectural risk factor evaluated (Table 1).

All lesions without hemorrhagic presentation in the study were identified on SWI. The AUC of The deep or posterior fossa location detected by SWI were 1.

SWI were a sensitive approach for detecting draining veins of bAVM. On detecting deep exclusive venous drainage, SWI was 92% sensitive and 95% specific. On detecting venous

ectasia and venous varices, SWI was 91% and 93% sensitive and 97% and 0.97% specific, respectively. In four patients, additional superficial draining veins into the superior sagittal sinus and into the transverse sinus were identified on DSA but were missed on SWI by both readers (Figure 1). Depiction of an additional draining vein on DSA changed the general interpretation of venous drainage pattern in two patients. But no deep drainage vein was missed on SWI.

A total of 6 aneurysms were visualized on DSA, of which two were in the course of the feeding artery of bAVM and one was intranidal aneurysm, the others were not associated aneurysms (Figure 2). On SWI, all aneurysms were identified except one associated aneurysm.

In seven of 81 patients, SWI did not identify additional small arterial feeders of the bAVM that were retrospectively seen only on DSA.

On SWI, 39 patients (48.15%) were detected with silent intralesional microhemorrahge. In 15 patients, silent microhemorrahge was detected only on SWI, but no patients displayed silent microhemorrahge only on T2WI (Figure 3).

Within the patients without microhemorrhage (n = 42), the AUC of detection of angioarchitectural features including deep or posterior fossa location, deep exclusive venous drainage, venous ectasia, venous varices and the presence of associated aneurysm) on SWI were 1, 0.93, 0.93, 0.96, and 0.75, repectively. In the patients with microhemorrhage (n = 39), the AUC of detection of angioarchitectural features on SWI were 1, 0.93, 0.96, 0.86 and 1, respectively.

No significant difference ($P > 0.05$) was found in age at scan, the gender, and angioarchitectural characteristics between cases with and without silent microhemorrhage (Table 2).

Discussion

In this study, we demonstrate that SWI offers a unique imaging contrast without radiation exposure, allowing for a high sensitivities and specificities in depicting certain angioarchitectural characteristics in unruptured bAVM.

SWI uses the paramagnetic deoxy-Hb as an intrinsic contrast agent. Deoxyhemoglobin causes a reduction in T2* as well as a phase difference between the vessel and its surrounding parenchyma [21]. Hence, SWI is already known to be clinically useful in the evaluation of low-flow vascular malformations such as developmental venous anomalies, telangiectasias and cavernomas [12, 13, 22]. Recently, many researchers found that SWI can also be used to evaluate high shunt flow vascular malformations [23–25]. However, our study is the first to our knowledge to evaluate the angioarchitecture of bAVM by SWI in a large series of patients. Many studies suggested that certain angioarchitectural characteristics are associated with the risk of future hemorrhage[1, 6–9], so the evaluation of angioarchitecture of bAVM is very valuable for the weighting the risk of natural history and invasive intervention.

Ichiro et al [26] reported that the presence of SWI hyperintensity within the venous structure was a useful indicator of retrograde leptomeningeal venous drainage in patients with dural arterial venous fistulae. Jagadeesan et al [23] reported abnormally hyperintense SWI signal within the draining veins of bAVM with 93% sensitivity and 98% specificity, and Toshiteru [13] reported that magnitude SWI images depicted a larger number of draining veins in bAVM, even when hyperintensity in draining veins was not visualized on time-of-flight images. Our results confirm that SWI can reliably detect deep venous drainage in unruptured bAVM. The venous hyperintensity evident with SWI has been attributed to the time-of-flight phenomenon that is intrinsic to high-velocity arterial flow and to the lack of paramagnetic phase shift secondary to the diamagnetic oxyhemoglobin content of arterial blood[23, 24, 26].

Exclusive venous drainage as another hemorrhage risk factor of bAVM [1, 17,27,28] is still controversial. Of note, as we evaluated exclusive venous drainage, superficial draining veins were missed in four cases but no deep drainage vein was missed on SWI. This may because the superficial draining veins presented low signal intensity and were not ectasia in these cases, which means they could not be identified easily. The low signal intensity in draining veins was also described by Toshiteru et al [13]. This may have resulted from lower oxyhemoglobin content and pressure in vessels.

The risk of hemorrhage in patients with bAVM and associated aneurysms was reported to be 7% per year, which is greater than the 3% risk of hemorrhage for patients with only bAVM [3, 29]. In our study, two flow-related aneurysms were identified but the intranidal aneurysm was missed. The one reason is because SWI was a 2D imaging method, and it can not be reformatted into a 3D images which may demonstrate associated aneurysms more clearly. The other reason is that some associated aneurysms are really hard to detect even in DSA because of the tortuous vessels surrounding them.

Silent intralesional microhemorrhage was evaluated on SWI in our study. Higher flow velocities coupled with an abnormal blood-brain barrier may contribute to extravasation of red blood cells into the surrounding brain and explain the hemosiderin occasionally seen around bAVM [31]. As a confounding factor, silent intralesional microhemorrhage did not impair the diagnostic accuracy for each angioarchitectural risk factor evaluated on SWI. Recently, some studies have found that silent intralesional microhemorrahge could be considered in risk evaluation [6, 7]. Our unpublished work shows SWI is sensitive in detecting intralesional microhemorrahge and suggests good correspondence correlating with histological examination. Hence, SWI may have the potential of integrated evaluation of bAVM, both in angioarchitectural characteristics and in detection of microhemorrahge, which is what we are going to explore next.

There are several limitations to our study. First, the data reported was retrospective in nature. Only patients with natural history were included in our study. The diagnostic performance of SWI in cases with preoperative embolization or radiosurgery remains unclear. Second, our study did not elucidate the reason of signal intensity of draining veins that showed mixed intensity or hypointensity in bAVM. One study suggested that this might be due to a dephasing effect caused by the long TE of the sequence and high flow of the vein [13]. The exact explaination of signal intensity of abnormal veins on SWI in the setting of AVM is

also unclear and requires further study. A correlative study between SWI and hemodynamic analysis of bAVM may be useful in this regard.

CONCLUSIONS

SWI was useful for the assessment of numerous unruptured bAVM angioarchitectural characteristics. It might be a promising non-invasive technique for assessing angioarchitectural features of unruptured bAVM, which provides an alternative in future prospective study and follow-up of patients with unruptured bAVM.

Acknowledgments

Funding: This work was supported by the National Institutes of Health [grant number R01 NS034949]; National Natural Science Foundation of China [grant number H0906 81271313 and H0906 81571110]; China Scholarship Council [grant number 201508110252].

3) Funding: This work was supported by the National Institutes of Health [**R01 NS034949 to Helen Kim**]; National Natural Science Foundation of China [**H0906 81271313** and **H0906 81571110** to **Y.L. Zhao**]; China Scholarship Council [**No. 201508110252** to **L. Ma**] in data collection.

Abbreviations list

bAVM	Brain arteriovenous malformation
SWI	Susceptibility weighted image
T2WI	T2-weighted images
DSA	Digital subtraction angiography
CI	Confidence interval
Se	Sensitivity
Sp	Specificity
PPV	Predictive positive value
NPV	Negative predictive value
AUC	Area under receiver operating curve

References

1. Geibprasert S, Pongpech S, Jiarakongmun P, Shroff MM, Armstrong DC, Krings T. Radiologic assessment of brain arteriovenous malformations: what clinicians need to know. Radiographics 2010;30:483–501. [PubMed: 20228330]
2. Gross BA, Du R. Natural history of cerebral arteriovenous malformations: a meta-analysis. J Neurosurg. 2013;118:437–443. [PubMed: 23198804]
3. Lv X, Li Y, Yang X, Jiang C, Wu Z. Characteristics of arteriovenous malformations associated with cerebral aneurysms. World Neurosurg. 2011;76:288–291. [PubMed: 21986426]
4. Hartmann A, Mast H, Mohr JP, Dandie G.Morbidity of intracranial hemorrhage in patients with cerebral arteriovenous malformation. Stroke.1988;29:931–934.

5. Berman MF, Sciacca RR, Pile-Spellman, Stapf C, Connolly ES Jr, Mohr JP, et al. The epidemiology of brain arteriovenous malformations. Neurosurgery.2000;47:389–396; discussion 397. [PubMed: 10942012]
6. Guo Y, Saunders T, Su H, Kim H, Akkoc D, Saloner DA, et al., Silent intralesional microhemorrhage as a risk factor for brain arteriovenous malformation rupture. Stroke. 2012;43:1240–1246. [PubMed: 22308253]
7. Abla AA, Nelson J, Kim H, Hess CP, Tihan T, Lawton MT. Silent arteriovenous malformation hemorrhage and the recognition of “unruptured” arteriovenous malformation patients who benefit from surgical intervention. Neurosurgery.2015;76:592–600. [PubMed: 25714514]
8. da Costa L, Wallace MC, Ter Brugge KG, O’Kelly C, Willinsky RA, Tymianski M. The natural history and predictive features of hemorrhage from brain arteriovenous malformations. Stroke. 2009;40:100–105. [PubMed: 19008469]
9. Lai LF, Chen JX, Zheng K, He XY, Li XF, Zhang X, et al. Posterior fossa brain arteriovenous malformations : Clinical features and outcomes of endovascular embolization, adjuvant microsurgery and radiosurgery. Clin Neuroradiol. 2018;28:17–24. [PubMed: 27154219]
10. Abecassis IJ, Xu DS, Batjer HH, Bendok BR.Natural history of brain arteriovenous malformations: a systematic review. Neurosurg Focus.2014;37:E7.
11. Hadizadeh DR, von Falkenhausen M, Gieseke J, Meyer B, Urbach H, et al. Cerebral arteriovenous malformation: Spetzler-Martin classification at subsecond-temporal-resolution four-dimensional MR angiography compared with that at DSA. Radiology.2008;246:205–213. [PubMed: 17951352]
12. Wrede KH, Dammann P, Johst S, Mönninghoff C, Schlamann M, Maderwald S,et al., Non-Enhanced MR Imaging of Cerebral Arteriovenous Malformations at 7 Tesla. Eur Radiol. 2006;26:829–839.
13. Miyasaka T, Taoka T, Nakagawa H, Wada T, Takayama K, Myochin K et al. Application of susceptibility weighted imaging (SWI) for evaluation of draining veins of arteriovenous malformation: utility of magnitude images. Neuroradiology.2012;54:1221–1227. [PubMed: 22592320]
14. Haacke EM, Mittal S, Wu Z, Neelavalli J, Cheng YC. Susceptibility-weighted imaging: technical aspects and clinical applications, part 1. AJNR Am J Neuroradiol.2009;30:19–30. [PubMed: 19039041]
15. Mittal S, Wu Z, Neelavalli J, Haacke EM. Susceptibility-weighted imaging: technical aspects and clinical applications, part 2. AJNR Am J Neuroradiol.2009;30:232–252. [PubMed: 19131406]
16. Thomas B, Somasundaram S, Thamburaj K, Kesavadas C, Gupta AK, Bodhey NK,et al. Clinical applications of susceptibility weighted MR imaging of the brain - a pictorial review. Neuroradiology.2008;50:105–116. [PubMed: 17929005]
17. Ma L, Chen XL, Chen Y, Wu CX, Ma J, Zhao YL. Subsequent haemorrhage in children with untreated brain arteriovenous malformation: Higher risk with unbalanced inflow and outflow angioarchitecture. Eur Radiol.2017;27(7):2868–2876. [PubMed: 27900505]
18. Taeshineetanakul P, Krings T, Geibprasert S, Menezes R, Agid R, Terbrugge KG, et al. Angioarchitecture determines obliteration rate after radiosurgery in brain arteriovenous malformations. Neurosurgery.2012;71:1071–1078; discussion 1079. [PubMed: 22922676]
19. Atkinson RP, Awad IA, Batjer HH, et al. Reporting terminology for brain arteriovenous malformation clinical and radiographic features for use in clinical trials. Stroke.2001;32:1430–1442. [PubMed: 11387510]
20. Kim H, Al-Shahi Salman R, McCulloch CE, Stapf C, Young WL. Untreated brain arteriovenous malformation: patient-level meta-analysis of hemorrhage predictors. Neurology.2014;83:590–597. [PubMed: 25015366]
21. Reichenbach JR, Venkatesan R, Schillinger DJ, Kido DK, Haacke EM. Small vessels in the human brain: MR venography with deoxyhemoglobin as an intrinsic contrast agent. Radiology. 1997;204:272–277. [PubMed: 9205259]
22. Jagadeesan BD, Cross DT 3rd, Delgado Almandoz JE, Derdeyn CP, Loy DN, McKinstry RC, et al. Susceptibility-weighted imaging: a new tool in the diagnosis and evaluation of abnormalities of the vein of Galen in children. AJNR Am J Neuroradiol.2012;33:1747–1751. [PubMed: 22517286]

23. Jagadeesan BD, Delgado Almandoz JE, Moran CJ, Benzinger TL. Accuracy of susceptibility-weighted imaging for the detection of arteriovenous shunting in vascular malformations of the brain. Stroke.2011;42:87–92. [PubMed: 21088245]
24. Jagadeesan BD, Delgado Almandoz JE, Benzinger TL, Moran CJ. Postcontrast susceptibility-weighted imaging: a novel technique for the detection of arteriovenous shunting in vascular malformations of the brain. Stroke.2011;42:3127–3131. [PubMed: 21940964]
25. Hodel J, Blanc R, Rodallec M, Guillonnet A, Gerber S, Pistocchi S, et al. Susceptibility-weighted angiography for the detection of high-flow intracranial vascular lesions: preliminary study. Eur Radiol.2013;23:1122–1130. [PubMed: 23111817]
26. Nakagawa I, Taoka T, Wada T, Nakagawa H, Sakamoto M, Kichikawa K, et al. The use of susceptibility-weighted imaging as an indicator of retrograde leptomeningeal venous drainage and venous congestion with dural arteriovenous fistula: diagnosis and follow-up after treatment. Neurosurgery.2013;72:47–54; discussion 55.
27. Kellner CP, McDowell MM, Phan MQ, Connolly ES, Lavine SD, Meyers PM,et al.Number and location of draining veins in pediatric arteriovenous malformations: association with hemorrhage. J Neurosurg Pediatr.2014;14:538–545. [PubMed: 25238624]
28. Ellis MJ, Armstrong D, Vachhrajani S, Kulkarni AV, Dirks PB, Drake JM, et al. Angioarchitectural features associated with hemorrhagic presentation in pediatric cerebral arteriovenous malformations. J Neurointerv Surg.2013;5:191–195. [PubMed: 22416111]
29. Lai LF, Chen M, Chen JX, Zheng K, He XY, Li XF, et al. Fistula and Infratentorial Location, Characteristics That Contribute to Cerebral Arteriovenous Malformations, Lead to the Formation of Associated Aneurysms in Patients. World Neurosurg.2016;88:510–8. [PubMed: 26520431]
30. Stapf C, Mast H, Sciacca RR, Choi JH, Khaw AV, Connolly ES, et al. Predictors of hemorrhage in patients with untreated brain arteriovenous malformation. Neurology.2006;66:1350–1355. [PubMed: 16682666]
31. Xiaolin C, Daniel C, David S, Nelson J, Su H, Lawton MT, et al. Higher Flow Is Present in Unruptured Arteriovenous Malformations With Silent Intralesional Microhemorrhages. Stroke. 2017; 48:2881–2884. [PubMed: 28855391]

Highlights

- SWI offers new perspectives for detecting angioarchitectural risk factors of unruptured bAVM.
- SWI can detect silent intralesional microhemorrahge in unruptured bAVM sensitively.
- Silent intralesional microhemorrhage did not impair the diagnostic accuracy for each angioarchitectural risk factor evaluated on SWI.

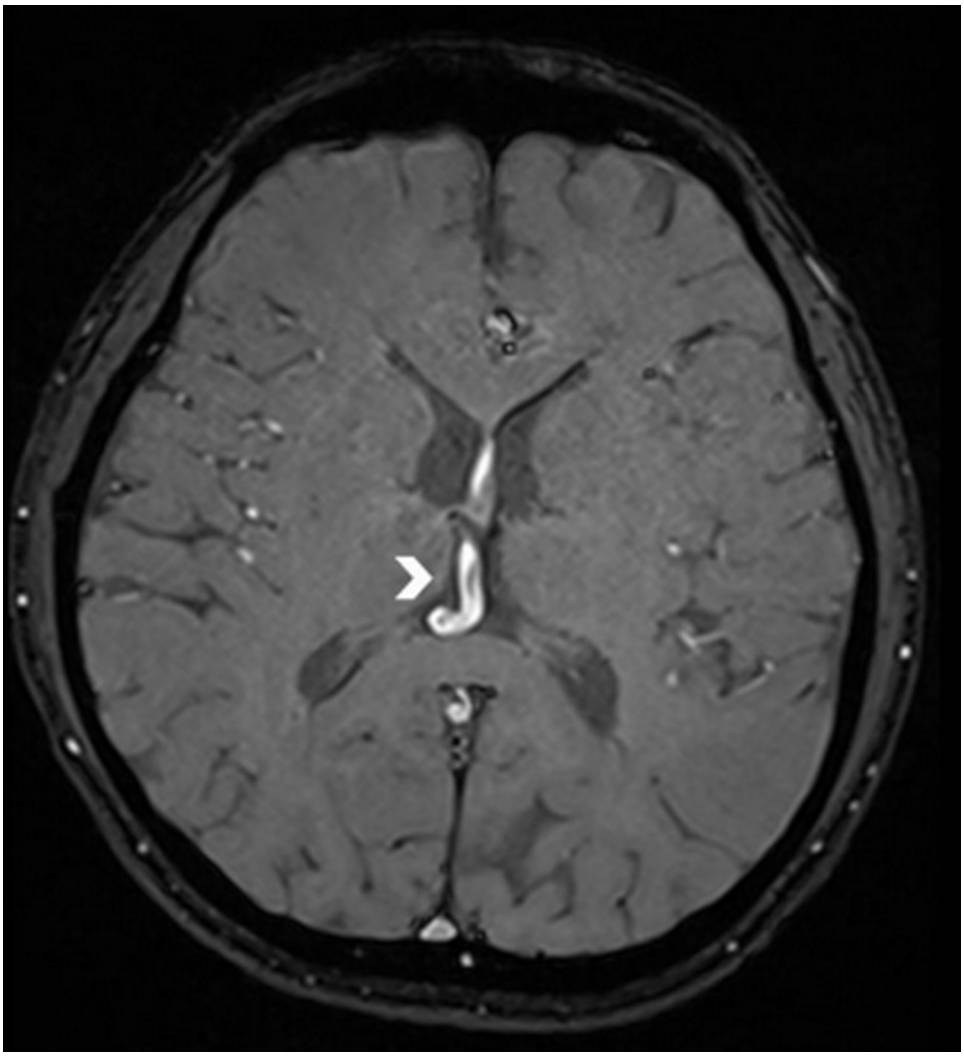

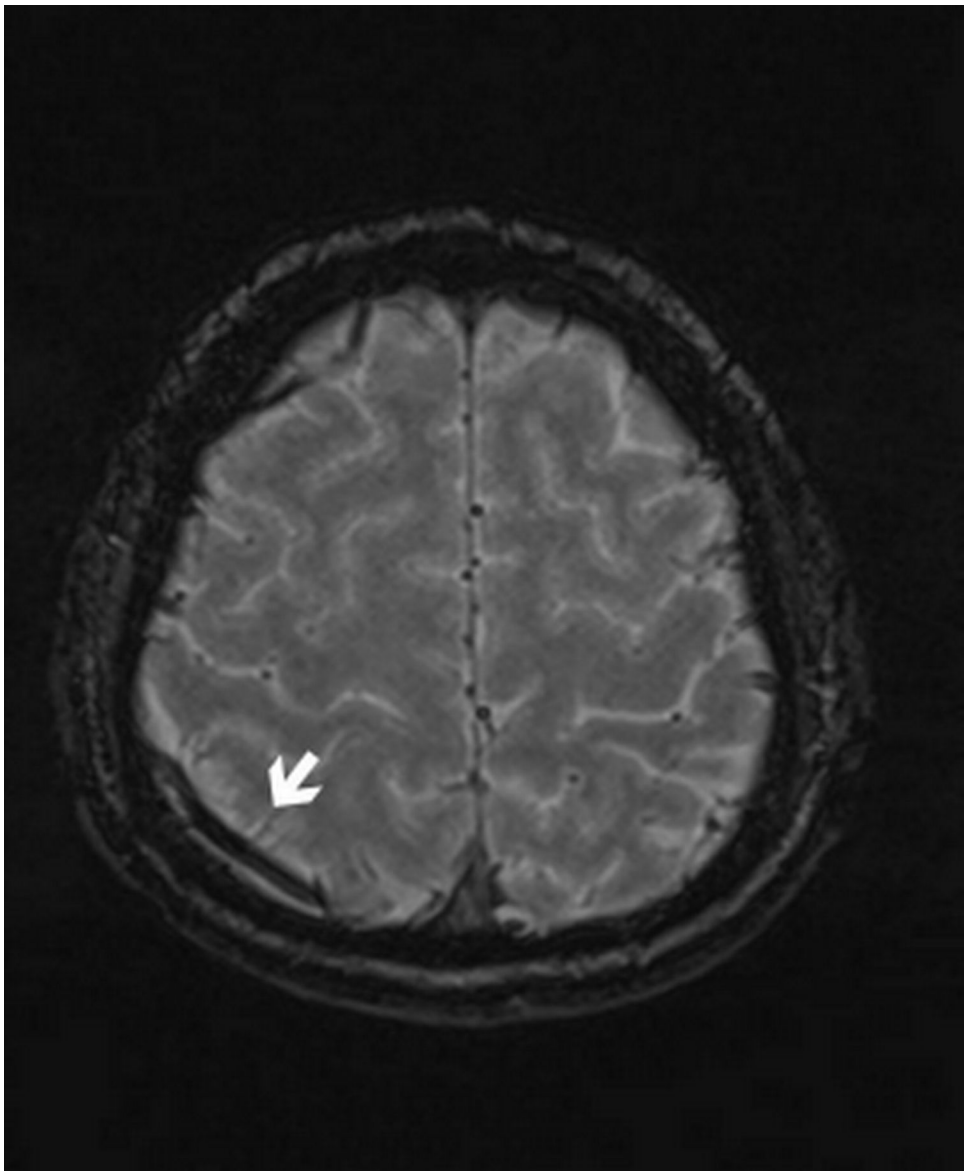

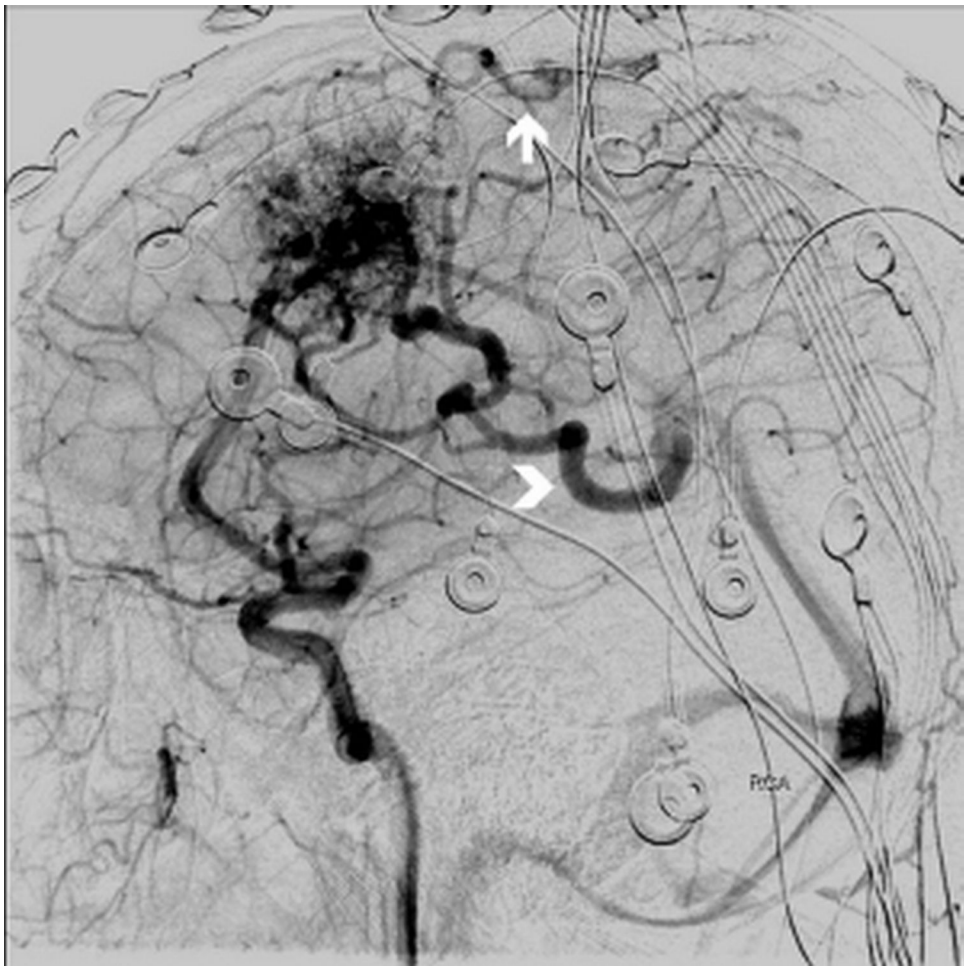

Figure 1. Identification of draining veins of bAVM on SWI

A 37 year-old man with headache. A, Axial SWI demonstrates the deep draining vein (arrowhead). B. Axial SWI demonstrates one of the superficial draining veins, which is missed by both two readers. Notice the draining vein is not dialated and shows hypointensity, which is like a normal cortical vein (white arrow). C, Right internal carotid angiography shows the superficial draining vein (white arrow) and the deep draining vein (arrowhead).

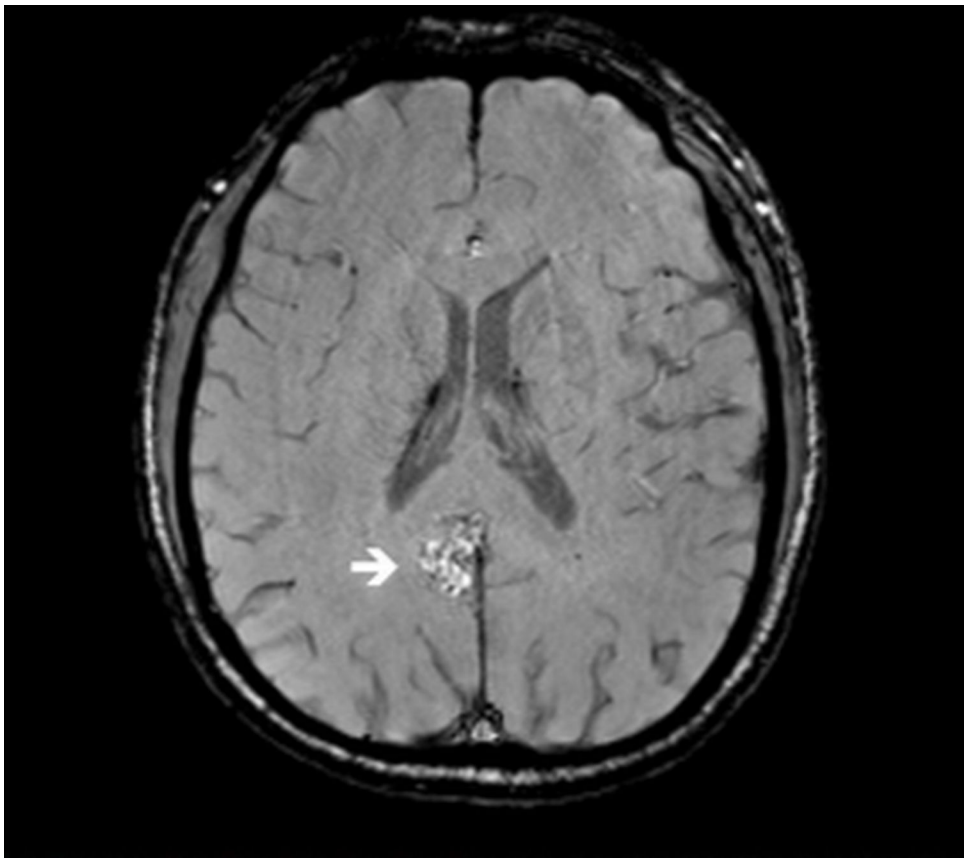

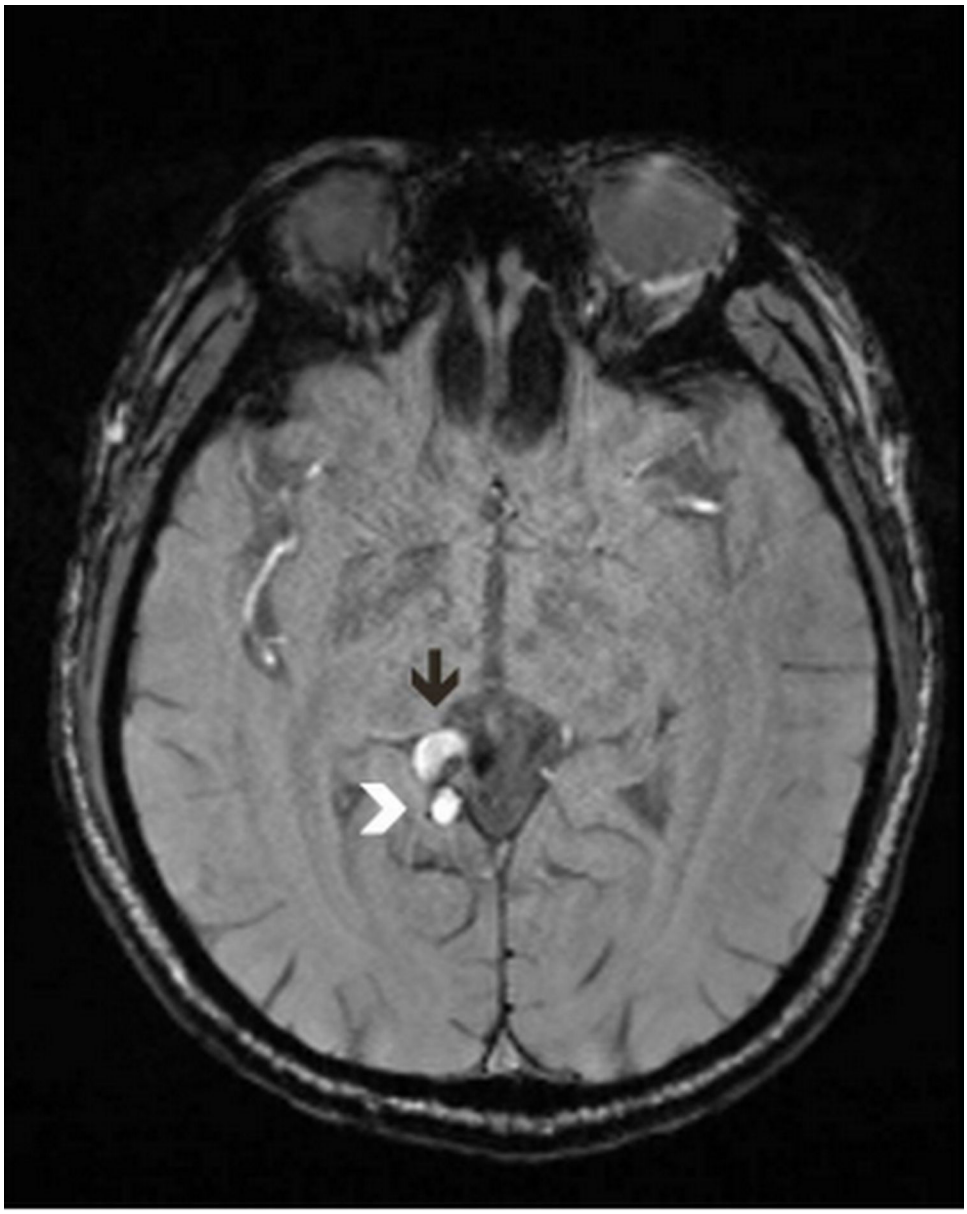

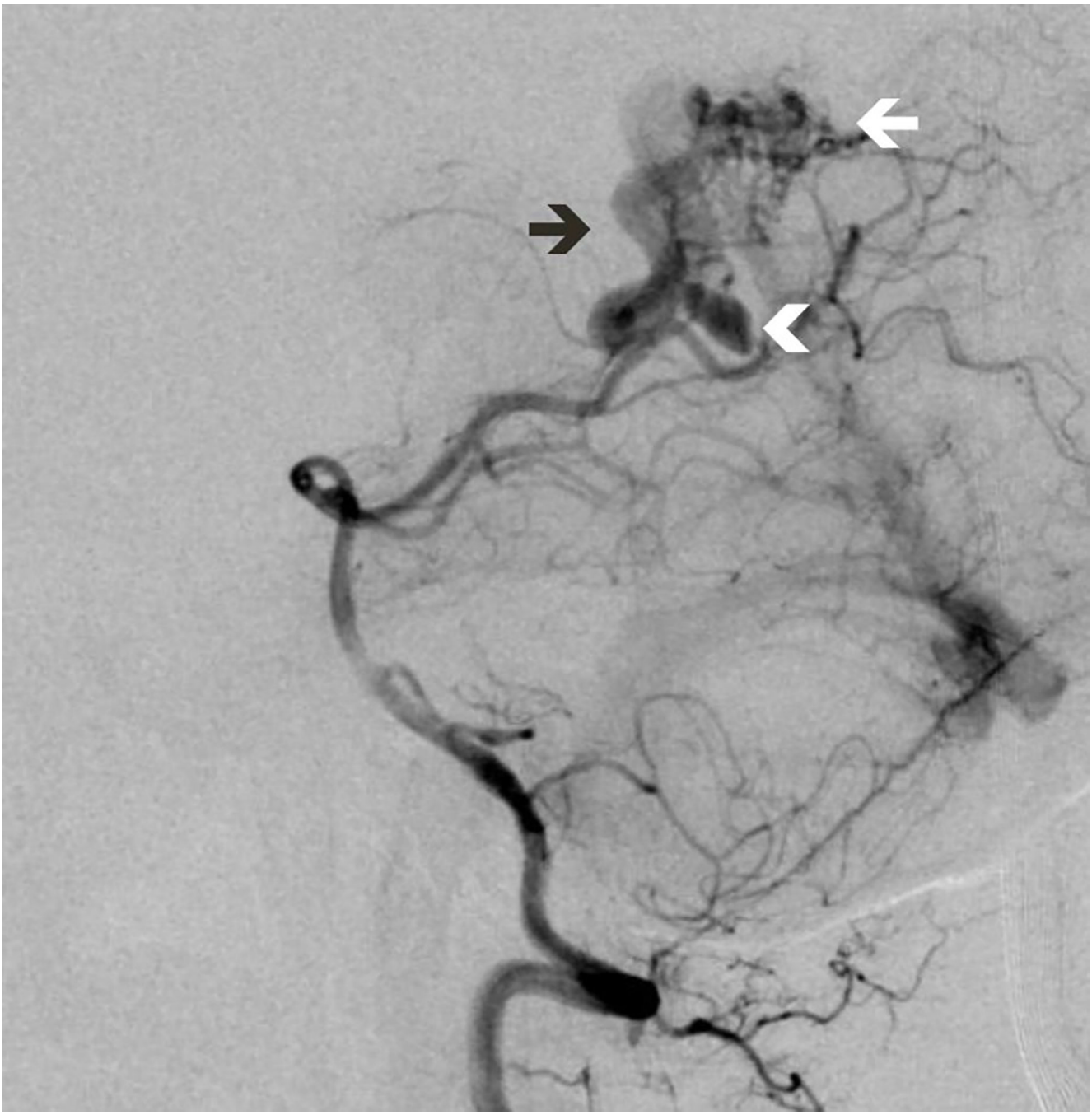

Figure 2. Identification of associated aneurysm of bAVM on SWI

A 54 year-old man with dizziness. A. Axial SWI demonstrates the nidus (white arrow). B. Another slice of SWI shows the draining vein (black arrow) and the associated aneurysm (arrowhead) behind it. C. Right internal carotid angiography confirms the nidus (white arrow), the draining vein (black arrow) and the associated aneurysm (arrowhead). D. The associated aneurysm was embolized with micro-coils (arrowhead).

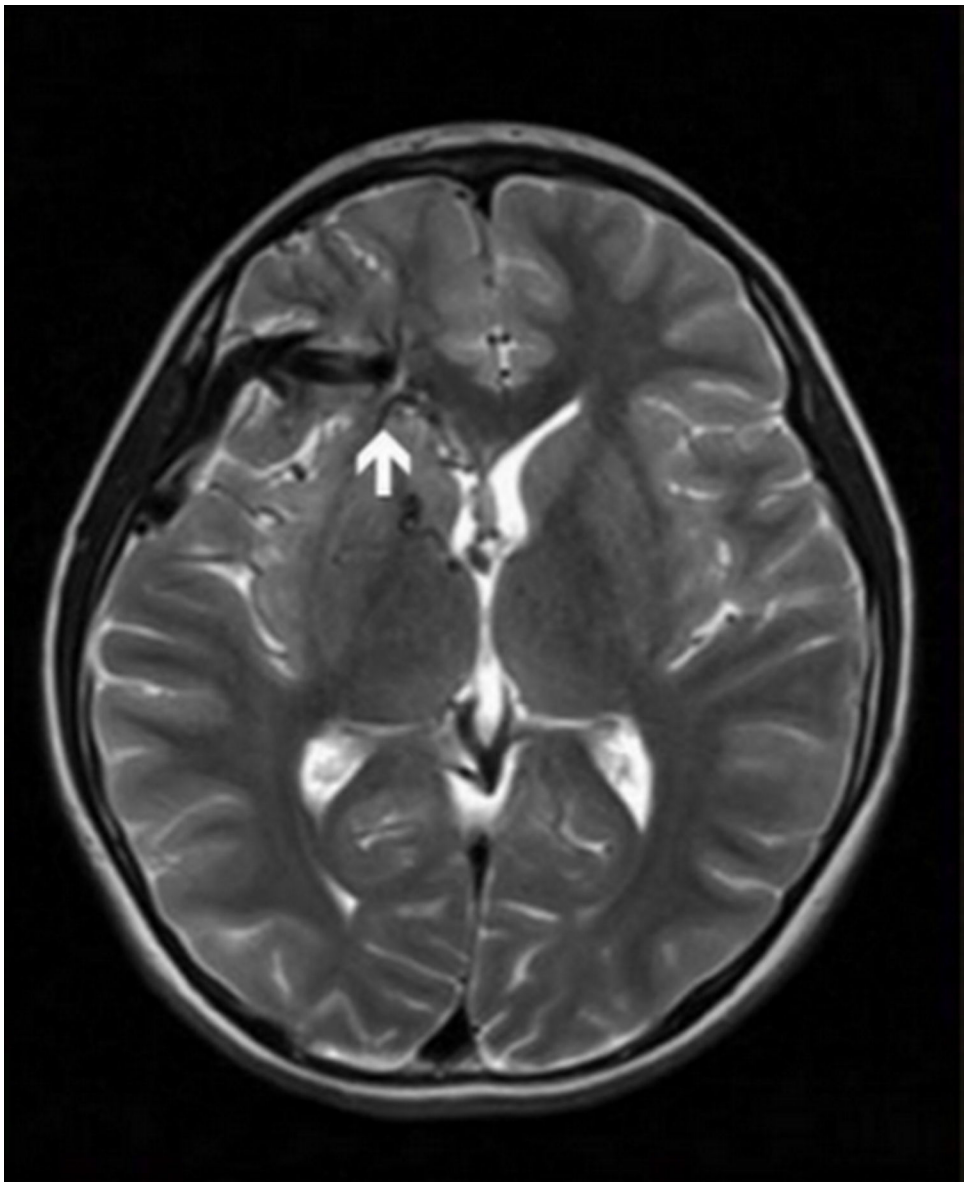

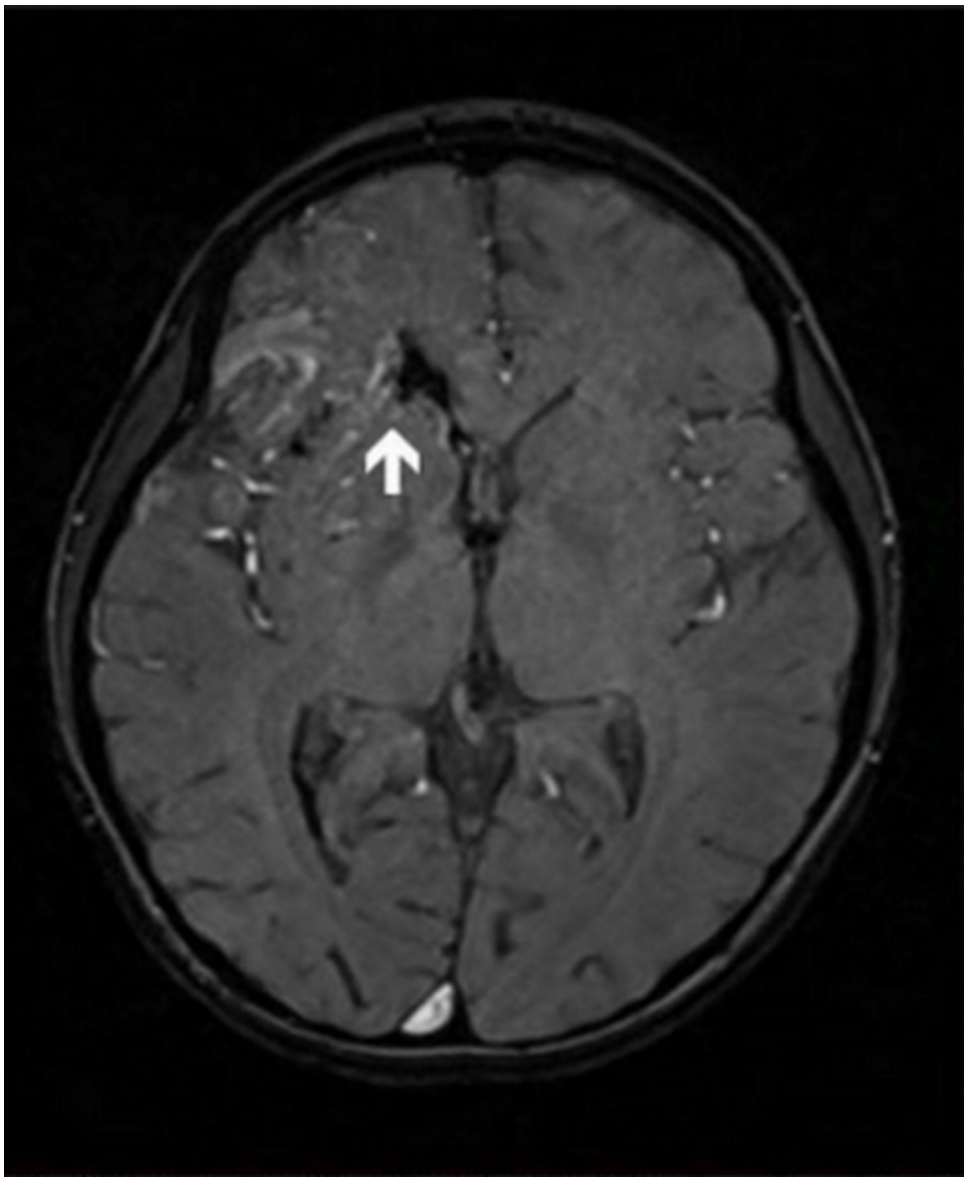

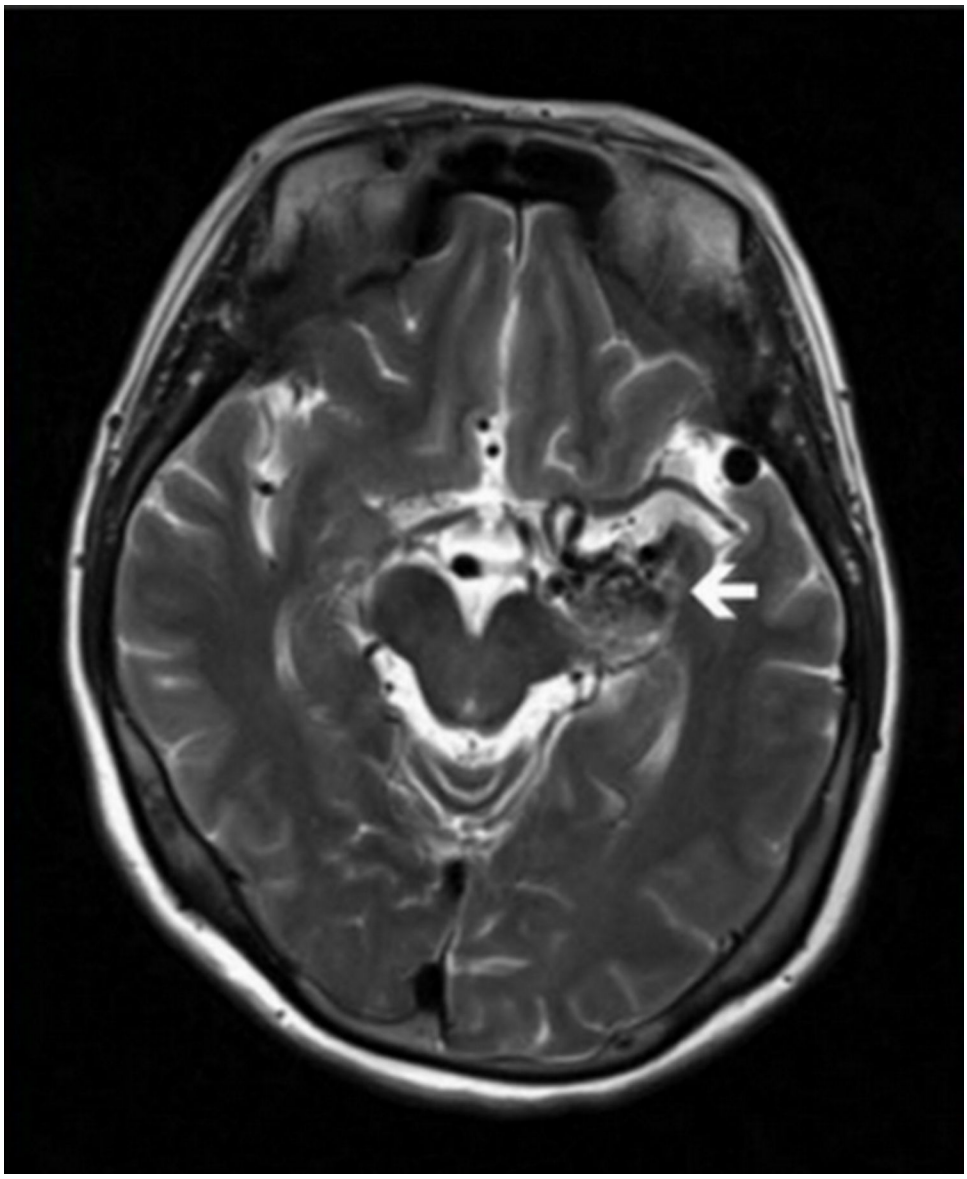

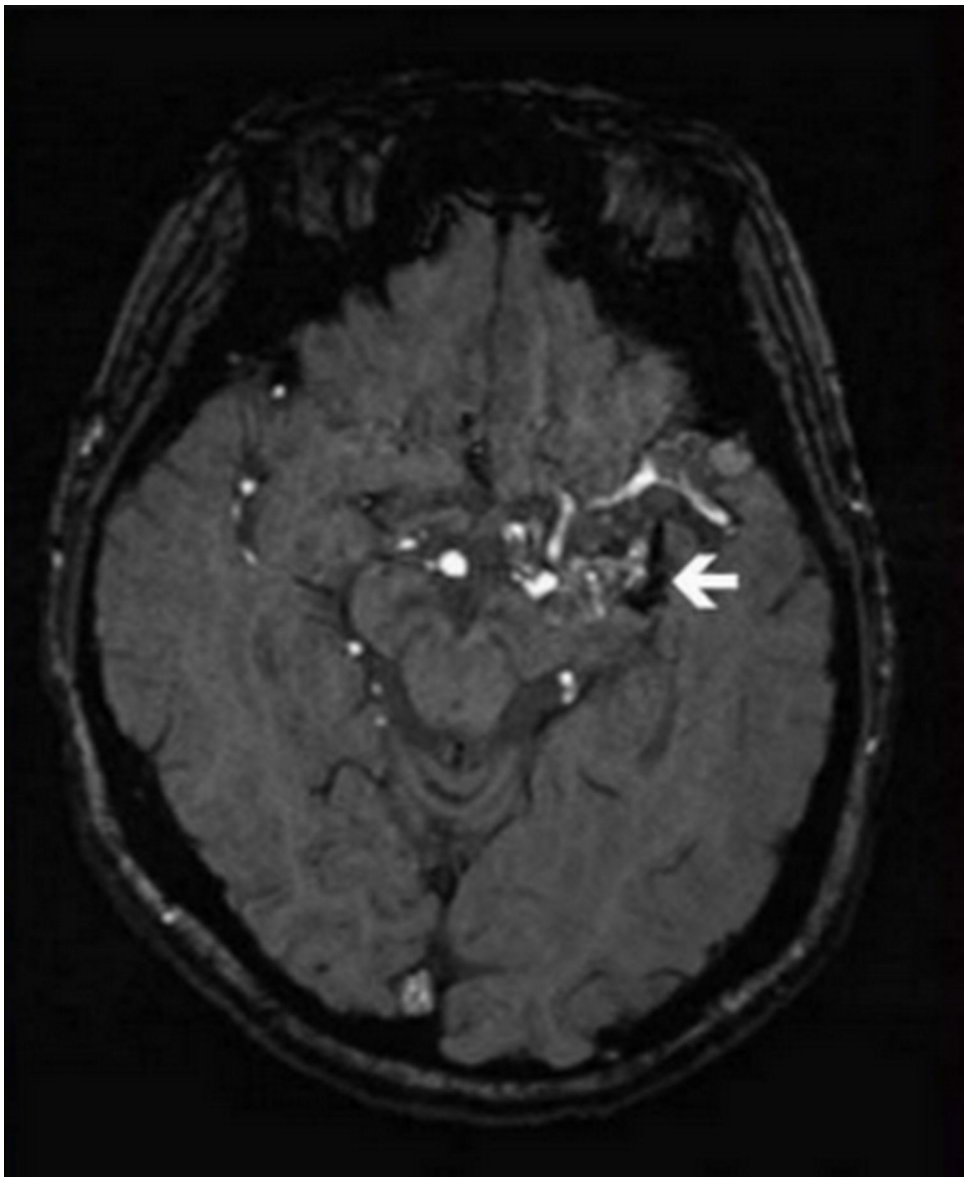

Figure 3. Silent intralesional microhemorrahge of bAVM on T2WI and SWI

A, A 10 year-old boy with unruptured bAVM of right frontal lobe. T2WI shows nidus and enlarged draining vein, with no silent intralesional microhemorrahge (arrow). B, SWI of the same patient shows silent microhemorrahge clearly beside right ventricular anterior horn (arrow). C, A 58 year-old woman with unruptured bAVM of left hippocampus. The silent microhemorrahge adjacent to the nidus was equivocal on T2WI. D, SWI of the same patient shows silent microhemorrahge clearly (arrow).

Table 1

Accuracy of SWI for the detection of angioarchitectural features of unruptured bAVM

Characteristic (nSWI / nDSA)	Diagnostic Accuracy Parameters				
	Se (95% CI)	Sp (95% CI)	PPV (95% CI)	NPV (95% CI)	AUC (95% CI)
Deep or posterior fossa location (32/32)	1 (1–1)	1 (1–1)	1 (1–1)	1 (1–1)	1 (1–1)
Deep exclusive venous drainage (23/25)	0.92 (0.83–1)	0.95 (0.81–0.99)	0.89 (0.79–0.96)	0.97 (0.87–0.98)	0.93 (0.86–1)
Venous ectasia (41/45)	0.91 (0.88–0.99)	0.97 (0.96–1)	0.98 (0.95–1)	0.90 (0.88–1)	0.94 (0.91–1)
Venous varices (14/15)	0.93 (0.87–1)	0.97 (0.96–1)	0.88 (0.89–0.97)	0.99 (0.90–1)	0.95 (0.88–1)
Associated aneurysms (2/3)	0.67 (0.61–0.90)	1 (0.93–1)	1 (0.91–1)	0.99 (0.90–1)	0.83 (0.51–1)

CI indicates confidence interval; Se, sensitivity; Sp, specificity; PPV, predictive positive value; NPV, negative predictive value; AUC, area under receiver operating curve. nSWI and nDSA, No. of patients with certain characteristic detected by SWI and DSA.

Table 2

Characteristics of patients with and without silent intralesional microhemorrahge on SWI

Characteristic	Total (n = 81)	Silent intralesional microhemorrahge (+) (n = 39)	Silent intralesional microhemorrahge (−) (n = 42)	*F* value	*P* value
Gender (Female)	32 (43.21)	16 (41.03)	19 (45.24)	-	0.600
Age (y)	30.47±15.98	31.95±18.61	29.02±12.98	−0.378	0.705
Deep or posterior fossa location	32 (39.50)	18 (46.15)	14 (33.33)	-	0.475
Deep exclusivevenous drainage	25 (30.86)	15 (38.46)	10 (23.81)	-	0.229
Venous ectasia	45 (55.56)	23 (58.97)	22 (52.38)	-	0.482
Venous varices	15 (18.52)	4 (10.26)	11(26.19)	-	0.088
Associated aneurysms	3 (3.70)	1 (2.56)	2 (4.76)	-	0.603
Maximal nidus size (mm)	38.04±12.03	33.50±11.81	42.25±14.30	−0.357	0.644

Table entries are No. (%) or mean ± SD